The Journal of Immunology

Complement C3b/C3d and Cell Surface Polyanions Are Recognized by Overlapping Binding Sites on the Most Carboxyl-Terminal Domain of Complement Factor H

Jens Hellwage, T. Sakari Jokiranta, Manuel A. Friese, Tobias U. Wolk, Eva Kampen, Peter F. Zipfel and Seppo Meri

J Immunol 2002; 169:6935-6944; ;
doi: 10.4049/jimmunol.169.12.6935
http://www.jimmunol.org/content/169/12/6935

The Journal of Immunology is published twice each month by
The American Association of Immunologists, Inc.,
1451 Rockville Pike, Suite 650, Rockville, MD 20852

Print ISSN: 0022-1767 Online ISSN: 1550-6606.

Complement C3b/C3d and Cell Surface Polyanions Are Recognized by Overlapping Binding Sites on the Most Carboxyl-Terminal Domain of Complement Factor H[1]

Jens Hellwage,[2,3]*† T. Sakari Jokiranta,[2]* Manuel A. Friese,‡ Tobias U. Wolk,‡ Eva Kampen,‡ Peter F. Zipfel,†‡ and Seppo Meri*

Factor H (FH) is a potent suppressor of the alternative pathway of C in plasma and when bound to sialic acid- or glycosaminoglycan-rich surfaces. Of the three interaction sites on FH for C3b, one interacts with the C3d part of C3b. In this study, we generated recombinant constructs of FH and FH-related proteins (FHR) to define the sites required for binding to C3d. In FH, the C3d-binding site was localized by surface plasmon resonance analysis to the most C-terminal short consensus repeat domain (SCR) 20. To identify amino acids of FH involved in binding to C3d and heparin, we compared the sequences of FH and FHRs and constructed a homology-based molecular model of SCR19–20 of FH. Subsequently, we created an SCR15–20 mutant with substitutions in five amino acids that were predicted to be involved in the binding interactions. These mutations reduced binding of the SCR15–20 construct to both C3b/C3d and heparin. Binding of the wild-type SCR15–20, but not the residual binding of the mutated SCR15–20, to C3d was inhibited by heparin. This indicates that the heparin- and C3d-binding sites are overlapping. Our results suggest that a region in the most C-terminal domain of FH is involved in target recognition by binding to C3b and surface polyanions. Mutations in this region, as recently reported in patients with familial hemolytic uremic syndrome, may lead to indiscriminatory C attack against self cells. ***The Journal of Immunology,*** **2002, 169: 6935–6944.**

The C system is an essential part of innate immunity. It is composed of ~35 proteins in plasma and on cell membranes that are involved in C activation or act as receptors or self-protective molecules. The main functions of C are to protect the human body against invading microorganisms, initiate inflammation, remove debris from plasma and tissues, and enhance cell-mediated immune responses (1). The C system can be activated by Abs via the classical pathway and by certain carbohydrates via the lectin pathway. In addition, C can be activated directly via the alternative pathway of C (AP).[4] The AP is unique in its spontaneous initiation and in its ability to attack particles, membranes, and cells which are not specifically protected against activation (2). Moreover, this pathway also amplifies activation initiated by the classical or the lectin pathway.

The key component of the alternative pathway is C3. The spontaneous hydrolysis of its thioester allows the covalent binding of activated C3 to practically any surface which is in contact with plasma (3–5). After formation of the initial C3 convertases, AP activation proceeds via an amplification cascade and leads to effective opsonization of target structures with C3b. This process is followed by activation of phagocytes and formation of membrane attack complexes, which can result in phagocytosis and cell lysis, respectively (6). The activation of the alternative pathway is controlled at the level of C3b by the plasma protein factor H (FH) and by three membrane-bound regulators CD35, CD46, and CD55 (7, 8). The regulator FH is composed of 20 domains called short consensus repeats (SCR) or C control protein modules. Each SCR contains ~60 aa, maintained in a bead-like structure by two disulfide bridges (9, 10). FH regulates C activation by competing with factor B for binding to C3b, by enhancing dissociation of the C3 convertase, C3bBb, and by acting as a cofactor for factor I in the proteolytic inactivation of C3b (11–14). Some of the described functions of FH are also mediated by its alternatively spliced variant FH-like protein 1 (15). FH is practically the only regulator that is involved in protecting self structures which lack the membrane-bound regulators. For example, basement membranes in the kidney glomeruli require FH for their protection, and disturbances in AP regulation lead to membranoproliferative glomerulonephritis type II (16, 17). Overactivation of the AP can be caused by an inherited deficiency in FH (18, 19) or a functional inactivation of the protein (20). Recent reports have described that mutations in the FH gene associate with the familial (atypical) form of hemolytic uremic syndrome (HUS) (21–23). The majority of the reported mutations cluster to the C terminus of FH, particularly to the SCR20 domain.

FH is involved in the discrimination between activating (nonself) and nonactivating (self) structures. This ability depends on differential binding of FH to different types of surfaces to which C3b has become initially deposited (24–26). Nonactivator surfaces

*Department of Bacteriology and Immunology, Haartman Institute and Helsinki University Central Hospital, University of Helsinki, Helsinki, Finland; †Molecular Immunobiology Group and Department for Infection Biology, Hans Knoell Institute for Natural Products Research, Jena, Germany; and ‡Bernhard Nocht Institute for Tropical Medicine, Hamburg, Germany

Received for publication April 22, 2002. Accepted for publication October 15, 2002.

The costs of publication of this article were defrayed in part by the payment of page charges. This article must therefore be hereby marked *advertisement* in accordance with 18 U.S.C. Section 1734 solely to indicate this fact.

[1] This work was supported by the Academy of Finland, the Sigrid Jusélius Foundation, the Finnish Cancer Organizations, the Finnish Culture Foundation, State Subsidy for University Hospitals in Finland, the Deutscher Akademischer Austauschdienst (J.H. was a grantee of the Deutscher Akademischer Austauschdienst Hochschulsonderprogramm III), and the Deutsche Forschungsgemeinschaft (Project Zi432/5).

[2] J.H. and T.S.J. contributed equally to this work.

[3] Address correspondence and reprint requests to Dr. Jens Hellwage, Molecular Immunobiology Group, Hans Knoell Institute for Natural Products Research, Beutenbergstrasse. 11a, D-07745 Jena, Germany. E-mail address: hellwage@pmail.hki-jena.de

[4] Abbreviations used in this paper: AP, alternative pathway of C; FH, factor H; SCR, short consensus repeat domain; FHR, FH-related protein; HUS, hemolytic uremic syndrome; NMR, nuclear magnetic resonance; FH15–20 mut, FH15–20 mutant.

0022-1767/02/$02.00

like those of intact cells and the glomerular basement membranes contain negatively charged surface structures such as sialic acids and glycosaminoglycans. FH has binding sites for heparin at SCR7, SCR20, and possibly in the middle SCR12–15 region (27–30). Any of these sites may be relevant in the recognition of nonactivator structures, but their physiological roles have not yet been fully deciphered. In addition, three binding sites for the central component of C, C3b, have been characterized on FH. These have been mapped to the SCRs 1–4, 8–15, and 19–20 (31). The site on SCR19–20 interacts with the C3d region of C3b (31). The C terminus of FH can bind also to sialic acids on *Neisseria gonorrhoeae* and to the outer surface protein OspE of *Borrelia burgdorferi* (32, 33). This interaction probably contributes to the serum resistance of the pathogenic microbes.

FH is a member of a protein family which includes FH-like protein 1 and five FH-related proteins (FHRs) (34, 35). All members of this group of plasma proteins consist solely of SCR domains. The two most C-terminal domains of all five FHR proteins and of FH are highly similar in sequence. We have recently reported that also FHR-3 and FHR-4 bind to the C3d region of C3b (36). These FHRs lack a significant cofactor activity in the inactivation of C3b by factor I and have no decay-accelerating activity for the C3bBb complex. The fact that FH and possibly all FHR proteins have a C3d-binding site is intriguing but the physiological roles of the FHR proteins are not yet understood.

In light of the common features of the C-termini of FH and FHRs, the aim of this study was to locate and analyze the C3d-binding sites on FH and FHRs by generating recombinant constructs and analyzing their interactions by the surface plasmon resonance technique. Our results show that the most C-terminal domains of FH (SCR20) and FHR-3 (SCR5) are needed for the interaction with C3d. Based on similarity comparisons, we constructed a mutant of SCR15–20 of FH by replacing five residues in SCR20. The interactions of this mutant protein with C3d and heparin were reduced. Using homology-based molecular modeling, a three-dimensional structure model of the SCR19–20 of FH was generated. By docking analyses, putative binding sites on SCR20 for heparin and C3d were identified and a complementary site was identified on C3d, whose structure was recently solved by x-ray crystallography (37). Thus, we have identified the site and putative residues on FH, which are essential for the interaction of the C-terminal end of FH with C3d, C3b, and heparin. We demonstrate that the C3d- and heparin-binding sites overlap with each other. These results relate to the ability of the AP to discriminate between activating and nonactivating structures and help in understanding the pathogenesis of the familial form of the HUS.

Materials and Methods

Reagents and C components

Tosylamide-phenylethyl-chloromethyl-ketone-treated trypsin and soybean trypsin-chymotrypsin inhibitor were obtained from Sigma-Aldrich (St. Louis, MO). Soybean trypsin-chymotrypsin inhibitor was used at a ratio 1:3 (w/w) of trypsin to the inhibitor. The methods used for purifying FH, C3b, and C3d have been described previously (31, 38, 39). The purity of the proteins was >90% as confirmed by SDS-PAGE.

SDS-PAGE and Western blotting

Proteins were separated by SDS-PAGE with either 8% or 5–15% gradient minigels under nonreducing conditions using standard protocols. For immunoblotting, the proteins were transferred to nitrocellulose membranes (0.2 μm; Schleicher & Schuell, Dassel, Germany) (40). After blocking with 3% BSA, either polyclonal goat anti-FH IgG (Incstar, Stillwater, MN), rabbit anti-FHR-3, or anti-FHR-4 antiserum (41), all diluted 1/2000 in 2% skim milk, were used as primary Abs. As a secondary Ab, either alkaline phosphatase-conjugated rabbit anti-goat IgG Ab (1/2000 in 0.1% BSA-PBS; Zymed Laboratories, San Francisco, CA) or goat anti-rabbit Ig (1/2,000 in 0.1% BSA-PBS; Jackson ImmunoResearch Laboratories, West Grove, PA) was used. After three washing steps, the bound secondary Abs were detected by adding a standard substrate for the alkaline phosphatase.

Recombinant proteins

FHR-3, FHR-4, and the recombinant SCR15–20 construct of FH were cloned, expressed with the baculovirus system, and purified as described earlier (31, 41, 42). The recombinant constructs representing SCR1–3, 1–4, and 4–5 of FHR-3, SCR4–5 of FHR-4, and SCR15–19 of FH were generated using the expression vector pBSV-8His. For amplification of cDNA fragments, the following sequence-specific primers were used (restriction sites are shown in italics): FHR-3 SCR1 forward, TTT *CTG CAG* CAA GTG AAA CCT TGT GAT TTT CCA GA; FHR-3 SCR3 reverse, TTT *GAA TTC* AAT GCA AAT TGG TTG TGC TGA CCA TC; FHR-3 SCR4 forward, TTT *CTG CAG* AAT TCT TCA GAA AAG TGT GGA CCT CC; FHR-3 SCR4 reverse, TTT *GAA TTC* TAT GCA TCT AGG TGG TGC CGA CCA CT; FHR-3 SCR5 reverse, TTT *GAA TTC* TTC GCA TCT GGG GTA TTC CAC TAT CC; FHR-4 SCR4 forward, TTT *CTG CAG* AAT TCT TCA GAA AAG TGT GGG; FHR-4 SCR5 reverse, TTT *GAA TTC* TTC GCA TCT GGG GTA TTC CAC; FH SCR15 forward, *CTG CAG* GAA AAA ATT CCA TGT TCA CAA CCA CC; FH SCR19 reverse, TTT *GCG GCC GC*T AAG CAT TTT GGT GGT TCT GAC CAT T.

Site-directed mutagenesis of a putative heparin/C3d-binding site in SCR20 of FH

Amino acid mutations were introduced to a construct of SCR15–20 of FH using the QuikChange site-directed mutagenesis kit (Stratagene, Amsterdam, The Netherlands). The following primers were used: forward, GAG GGA TAT GAG CTT TCA TCA TCC TCT CAC ACA TTG CGA ACA AC, and reverse, GGA TGA TGA AAG CTC ATA TCC CTC TTT ACA CAC AAA TTC AAC TG for the mutations R1203E, R1206E, and R1210S; and forward, TCC GCC TAG AAT CAA TCA, and reverse, GGC GGA TGC ACA AGT TGG ATA CTC CA for the mutations K1230S and R1231A, respectively. The recombinant protein with the mutations was expressed in *Spodoptera frugiperda* insect cells using the pBSV-8His expression vector as described above. The mutations and sequences of the constructs were confirmed by DNA sequencing (Applied Biosystems, Weiterstadt, Germany).

Surface plasmon resonance-binding assays

Protein-protein interactions were analyzed by the surface plasmon resonance technique using Biacore 2000 and 3000 instruments (Biacore, Uppsala, Sweden) essentially as described earlier (31, 43). C3d was coupled via a standard amine-coupling procedure to the flowcells of a sensor chip (carboxylated dextran chip CM5; Biacore). Two flowcells were activated and C3d (50 μg/ml, dialyzed against 10 mM acetate buffer, pH 5.0) was first injected into one of the flowcells until an appropriate level of coupling for the binding experiments (>4000 resonance units) was reached. For kinetic analysis, the chip surface was coated with a lower density (~800 resonance units) of C3d. Unreacted groups were inactivated by ethanolamine-HCl injection. A control flowcell was prepared identically but without injecting a protein. Before the binding experiments, the flowcells were washed thoroughly with sequential injections of 2 M NaCl in 10 mM acetate buffer, pH 4.6 and 75 mM veronal-buffered saline, pH 7.4. FH, FHR-3, FHR-4, and a set of recombinant FHR constructs were dialyzed against the running buffer and the protein concentrations were measured using the Bicinchoninic Acid Protein Assay (Pierce, Rockford, IL). Each ligand was injected separately into the flowcell coupled with C3d and into a control flowcell using a flow rate of 5 μl/min at 22°C. The final concentrations of the fluid-phase ligands in the C3d binding assay (see Fig. 3) ranged from 100–125 μg/ml. Each binding interaction was assayed at least twice using independently prepared sensor chips. For kinetic analysis, the surface density of C3b/C3d was decreased to 800 surface plasmon resonance unit and the flow rate was raised to 20 μl/min. For the heparin inhibition series, binding of FH15–20 wild type and FH15–20 mutant (FH15–20 mut) to C3b was measured at a concentration of 100 μg/ml. Increasing concentrations of heparin (3–300 μg/ml, low m.w.; Sigma-Aldrich) were added to the analyte before the injection. For evaluating the difference in binding to C3d of the wild type vs the mutated protein, the half-life of the binding complex with C3b was calculated as described (43).

Heparin affinity chromatography

The recombinant proteins were diluted in an equilibration buffer (PBS, 50 mM NaCl) and applied onto a heparin column (1 ml HiTrap Heparin) using

an ÄKtaprime instrument (Amersham Pharmacia Biotech, Freiburg, Germany). The samples were passed twice over the column at a flow rate of 1 ml/min at 22°C and the fall-through was collected. After washing the column with 20 ml of equilibration buffer, the bound proteins were eluted with a linear NaCl gradient ranging from 50–500 mM. Fractions of 1 ml were collected and the column was regenerated with 5 ml of 1 M NaCl followed by 15 ml of equilibration buffer. The fractions were subjected to SDS-PAGE and Western blotting. Binding of the wild-type FH15–20 protein vs the mutated protein construct FH15–20 mut was tested in parallel. A small amount of ^{125}I-labeled mutated protein (representing ~20,000 cpm) was mixed with 30 μg of the unlabeled wild-type FH15–20 protein and subjected to affinity chromatography as described above. The experiment was repeated in the reverse setting with the radiolabeled wild-type and unlabeled mutant proteins. The chromatography was monitored by UV-detection (unlabeled protein) and detection of radioactivity (radiolabeled protein).

Sequence alignments

Two amino acid sequence alignments were made. First, the two most C-terminal SCRs of FH, FHR-3, and FHR-4 were aligned to create a consensus sequence. Second, SCRs 1–18 of FH were aligned to create a consensus sequence of residues found frequently in the SCR domain structure. The alignments were generated using the Jotun Hein method with the PAM250 residue weight table and DNAstar software (DNAstar, Madison, WI). The alignment of SCRs 1–18 of FH was corrected manually for a better overall alignment with SCR20. A criterion in the manual correction was a conservative location of amino acids close to (±3 residues) the four cysteines and the tyrosine ~20 residues forward from the first cysteine. In searching for amino acids corresponding to those found in SCRs 19–20, a mismatch of one position was accepted except for sequences spanning the least homologous areas (corresponding to residues 1169–1172, 1176–1183, and 1212–1216 of the FH sequence), where a mismatch of two positions was accepted. In all manual alignments and in constructing the consensus sequences, structurally related amino acids were considered comparable in the following groups: Lys and Arg, Asp and Glu, Asn and Gln, Ser and Thr, Phe and Tyr, Ala, Leu, Ile, and Val.

Molecular modeling of FH SCR19–20

A homology-based molecular model of FH SCR19–20 was established with the InsightII software (Biosym Technologies, San Diego, CA) using an O_2 workstation (Silicon Graphics, Mountain View, CA). The published nuclear magnetic resonance (NMR) structure of FH SCRs 15–16 (Brookhaven Protein Database accession code 1HFH) (44) was chosen as the template for modeling on the basis of highest homology. The Biopolymer module of InsightII was used to build a preliminary model of SCR19–20. For SCR19 one loop (residues 1118–1124) and for SCR20 five loops (residues 1162–1164, 1173–1179, 1184–1196, 1202–1213, and 1219–1221) were replaced using previously described criteria (45). After amino acid substitutions and energy minimization, the preliminary model structure was soaked in a waterbox (81.58 × 47.83 × 38.05 Å) of 4,274 water molecules to achieve an ~6 Å-thick layer of water around the whole protein as described previously (46). The energy minimizations were done using both the steepest descents and conjugate gradient algorithms until the maximum derivative was below 0.001 kcal/Å. Thereafter, molecular dynamics simulation was performed using a 14 Å cut-off and consistent valence force field as the force field (45). The target was simulated for 1 ps at 100 K and 92 ps at 300 K using a 1.0 fs time step throughout. Five structures were selected from the last 10 ps (at 300 K) according to their low potential energy and subjected to energy minimization in their waterboxes using the conjugate gradient algorithm. The structure with the lowest potential energy was chosen for further analyses. The respective coordinates have been deposited in the Brookhaven Protein Data Bank (PDB; accession code 1FHC). The model of the mutated FH SCR19–20 was constructed by replacing the five mutated amino acids to the above described model of the wild-type FH SCR19–20. The energy minimizations were performed as described above.

Docking analyses with the FH SCR19–20 model

The generated tertiary molecular model of FH wild-type SCR19–20 was subjected to two kinds of docking analyses. First, a manual docking was used to identify the best fitting sites on the surfaces of the FH SCR19–20 model and the recently described x-ray structure of C3d (PDB entry 1C3D) (37). The criteria for selecting the well-fitting corresponding surfaces were complementary contours, charges, and hydrophobicity of the surfaces. Second, docking analysis based on computer-aided energy minimization and molecular dynamics simulation was used to dock our model of FH SCR19–20 with the previously described NMR structure of heparin (PDB entry 1HPN) in six separate docking experiments. In each experiment heparin was positioned in a different way 5–15 Å away from the surface of SCR20: in front of, behind, above, below, and in two orientations (vertical and horizontal) laterally to the horizontally positioned FH SCR20. Starting from these positions, the heparin and SCR19–20 structures were subjected to steepest descents and conjugate gradient algorithms (until the maximum derivative was below 0.001 kcal/Å) and to a total of 40–50 ps dynamics simulation at 300 K (cutoff distance 50 Å) until the potential energy of the complex had reached a plateau level. The potential energies of each of the docking results were analyzed using the Analysis module of the InsightII program.

Results

Identification of the C3d-binding domains of FH and FHRs

The C inhibitor FH and the FHRs FHR-3 and FHR-4 all bind to C3d but the respective binding domains have not been known so far. The schematic structures of FH, FHR-3, and FHR-4 are shown in Fig. 1*A*. Sequence comparisons indicated that the two most C-terminal domains in all these proteins are highly conserved with >90% amino acid identity. To locate the putative C3d and heparin-binding sites within the SCR19–20 region of FH, we compared FH with the proteins FHR-3 and FHR-4 as "natural mutants" of the C terminus of FH. The following new recombinant constructs of FHR-3, FHR-4, and of the C-terminal part of FH were generated: SCR1–3, 1–4 and 4–5 of FHR-3, SCR4–5 of FHR-4, and SCR15–19 of FH (Fig. 1*B*). All constructs were purified by Ni^{2+}-chelation chromatography as described (42). In Western blotting analysis, a polyclonal anti-FHR-3 antiserum detected all the FHR-3 constructs, a polyclonal anti-FHR-4 antiserum detected the FHR-4 fragment, and a polyclonal anti-FH antiserum bound to the used FH mutants. In accordance with the close homology between members of the FH protein family the polyclonal anti-FHR-3 antiserum bound to FH, FHR-3, and FHR-4 (data not shown).

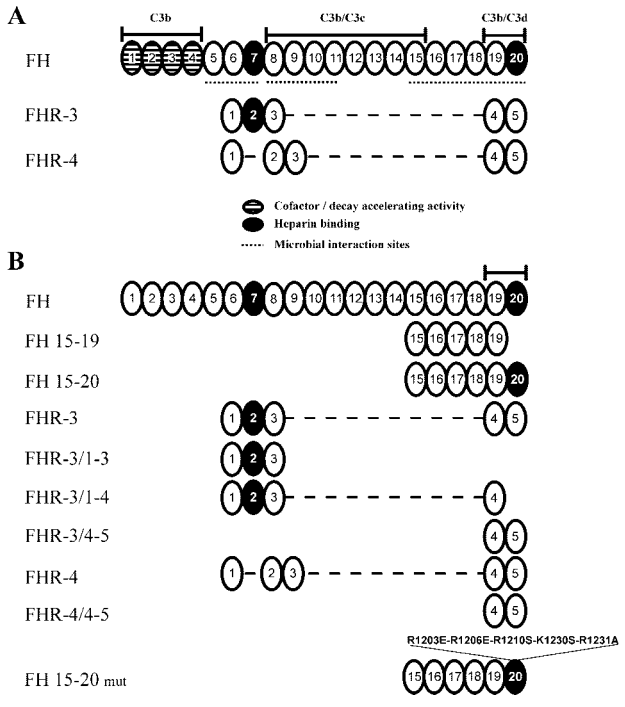

FIGURE 1. Schematic structure of FH, FHR-3, and FHR-4 (*A*) and the recombinant FH, FHR-3, and FHR-4 constructs used in this study (*B*). FH and the FHRs were aligned according to the level of homology between individual SCR domains. The SCRs within each protein are numbered consecutively. The binding sites for C3b and its cleavage fragments are shown according to Jokiranta et al. (31). The FH15–20 mut was generated by substituting the indicated positively charged residues in SCR20.

The recombinant constructs of FH, FHR-3, and FHR-4 were analyzed for their capacity to bind to C3d by the surface plasmon resonance technique. As positive controls we used FH purified from human plasma and the previously described recombinant FHR-3 and FHR-4 proteins (36). An association of the fluid-phase FH or FHR constructs with the immobilized C3d was detected as an increase in the resonance signal during the protein injection. The dissociation of the protein complex was followed after the injection. The constructs SCR4–5 of both FHR-3 and FHR-4 bound to C3d while the N-terminal constructs of FHR-3 (SCR1–3 and SCR1–4) did not (Figs. 2 and 3). The construct SCR15–19 of FH did not bind to C3d either (Fig. 4). Thus, the C3d-binding sites of FH and FHR-3 were located to the two most C-terminal domains of FH and FHR-3 and the interactions were found to require the most C-terminal domain SCR20 of FH and SCR5 of FHR-3, respectively.

Sequence analysis of the FH SCR20 domain

Because the C3d-binding domains were deduced for FH (SCR20) and FHR-3 (SCR5), we next compared their primary structures to those in other SCR domains to see which residues could be involved in C3d binding. FH SCR20 and FHR-3 SCR5 share 37 residues (Fig. 5). Almost all the SCR domains of proteins in the FH family contain a number of conserved key residues (9, 47) and domains SCR1–18 of FH do not bind to C3d (31). Thus, we generated a consensus sequence for non-C3d-binding domains (SCRs 1–18) of FH and found a total of 13 residues that are located at the same position in at least 50% of those domains (Fig. 5). Because it is unlikely that these residues would be specifically involved in C3d binding, they were removed from the putative C3d-binding consensus sequence and 24 residues were left on the list of possible C3d-binding residues.

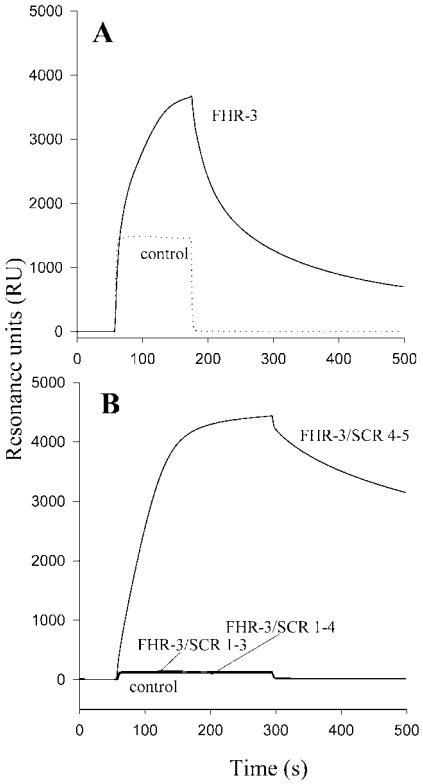

FIGURE 2. Binding of FHR-3 and its deletion mutants to C3d analyzed by surface plasmon resonance. The entire FHR-3 protein (*A*) and three recombinant constructs of FHR-3 comprising SCRs 1–3, 1–4, and 4–5 (*B*) were injected at a concentration of 100–125 μg/ml into a flowcell coupled with C3d (solid line) and into the control flowcell (blank channel, dotted line). In the control, only the bulk effects caused by ligands in the solution are seen. All recombinant constructs were tested on two different chip surfaces coated with C3d and representative figures are shown.

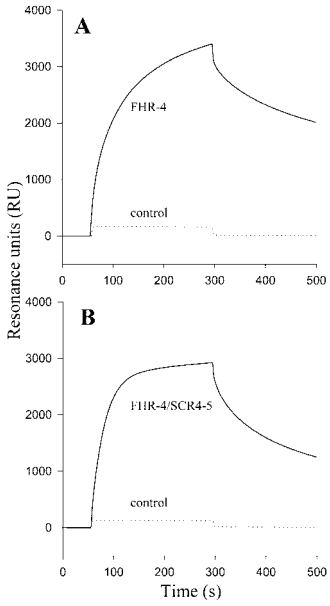

FIGURE 3. Binding of FHR-4 and its deletion mutant to C3d analyzed by surface plasmon resonance. The entire FHR-4 protein (*A*) and the FHR-4 SCR4–5 construct (*B*) were injected into a flowcell coupled with C3d (solid line) and into the control flowcell (dotted line) as described for Fig. 2.

Tertiary structure analysis of the putative C3d binding site on FH

To locate the putative C3d-binding residues in the tertiary structure of FH SCR20, a molecular model of SCR19–20 was constructed (Fig. 6). According to the sequence comparisons, a total of 24 residues was considered possibly involved in C3d binding (see previous paragraph). The positions of these residues in the tertiary molecular model structure of FH SCRs 19–20 showed that 12 of them formed a patch on the surface (V1168, I1169, S1170, E1172, M1174, N1178, L1181, R1182, K1202, L1223, E1224, and Y1225), while 12 other residues were scattered around the domain

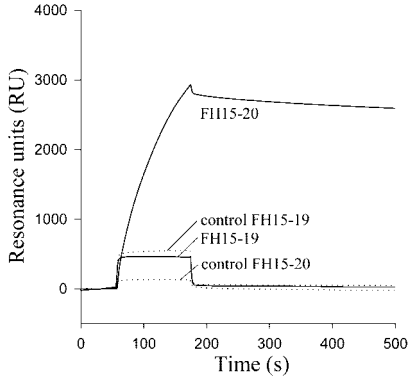

FIGURE 4. Binding of C-terminal constructs of FH to C3d analyzed by surface plasmon resonance. Recombinant constructs comprising SCR15–20 or SCR15–19 of FH were injected into a flowcell coupled with C3d (solid line) and into the control flowcell (dotted line). Although FH SCR15–20 binds strongly to C3d no binding of SCR15–19 was observed.

(Fig. 6*A*). In addition, P1226 common for FH SCR20 and FHR-3/4 SCR5 was located within the patch but is frequently found on other SCRs, too. Two residues found in FH but not in the FHR sequences were also located within the patch (R1171 and E1175). Three positively charged residues unique for FH were located next to the putative C3d-binding patch (R1210, K1230, and R1231).

The tertiary structure of C3d has been determined (37). Therefore, we were able to analyze by manual docking analysis in silico whether the patch of the putative C3d-binding residues on our model of FH had a suitable counterpart on the C3d structure (Fig. 7, *A* and *B*). The best fit in the docking analysis was obtained with a putative binding site that was distinct from the thioester site and the reported CD21-binding site on C3d (48). The identified putative FH-binding site consisted mainly of the C3d residues (the putative corresponding residues on the surface of FH SCR19–20 model are shown in parentheses) D223 (K1202), N225 (M1174), R226 (E1175), E228 (R1231), Q233 (Y1225, P1226), D254 (R1182), P258 (N1178, L1181), R261 (E1172), W262 (P1226), E265 (R1171), Q266 (Y1225), and R267 (E1224) as shown in Fig. 7*B*. The interacting area of C3d consists of the two peptide sequences of C3d (residues 219–240 and 254–267) suggested to be involved in FH binding in an earlier study (49).

Sequence analysis of the heparin-binding domain

One of the heparin-binding sites on FH is located at SCR20 (29, 30). Heparin is a highly negatively charged molecule and all the known heparin-binding sites of other proteins consist of positively charged residues. Neither FHR-3 nor FHR-4 binds to heparin with the C-terminal SCR4–5 (data not shown). Thus, we compared the positively charged residues in the primary structures of the SCR20 of FH and SCR5 of FHR-4. We found a total of nine basic residues on FH that were not found at the same location in the FHR-4 sequence and considered these as putative heparin-binding residues (Fig. 5).

Tertiary structure analysis of the putative heparin-binding site on FH

When the locations of the potential heparin-binding amino acid residues in the molecular model of FH SCR19–20 were analyzed, five of them were found to form a positively charged patch on the surface (R1203, R1206, R1210, K1230, and R1231) while the others (R1171, K1186, R1215, and K1222) were scattered around the domain. In addition, the positively charged patch included one residue (K1202) that was found also on FHR proteins which do not bind heparin. The putative role of the positively charged patch on SCR20 was analyzed by a series of computer-aided docking analyses. Docking was performed by positioning heparin close to the FH SCR19–20 model in six different orientations and subjecting the pairs of molecules to serial energy minimizations and molecular dynamics simulations (Fig. 7*C*). The potential energies of the structural complexes during the dynamics simulations were analyzed and, as expected, the potential energy dropped steeply in the beginning of the simulation at 300 Kcal and reached in each of the six simulations a plateau level at 1992–2264 Kcal. The lowest potential energy was reached when heparin was initially above the domain SCR20 (1992 Kcal). The corresponding structure after the dynamics simulation is shown in Fig. 7*C*. The analysis suggested that residues K1108 (SCR19), K1202, R1206, R1210, K1222, K1230, and R1231 are involved in heparin binding.

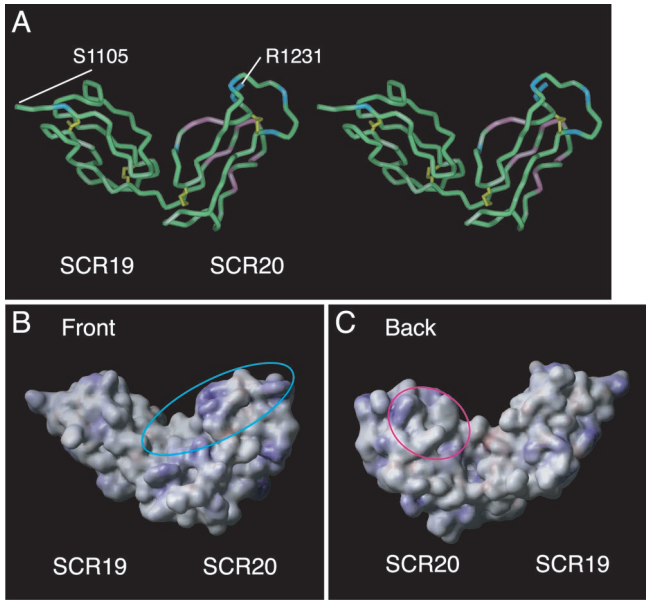

FIGURE 6. A tertiary molecular model of SCR19–20 of human FH. A homology model of FH SCR19–20 was generated using the NMR structure of FH SCR15–16 as a template (44). Energy minimizations and a total of 92 ps molecular dynamics simulations were performed at 300 K as described in *Materials and Methods*. *A*, Stereoview of the backbone of the model structure. The first and the last residue are marked and the cysteine bridges are shown in yellow. Backbone of the residues putatively responsible for heparin binding is shown in cyan and backbone of the residues putatively responsible for C3b/d binding in pink. *B* and *C*, charges on the surface of the FH SCR19–20 model. Positively charged surface areas are shown in blue and negatively charged surface areas in red. The putative heparin-binding site is indicated with a cyan oval and the putative C3b/d binding site with a pink oval.

Functional analysis of mutated FH SCR20

To test the functional contribution of the positively charged patch (K1202, R1203, R1206, R1210, K1230, and R1231) on the binding of FH to heparin, C3b, and C3d, five of the six positively charged amino acids were mutated in a construct FH SCR15–20. The following changes were introduced to generate the mutated

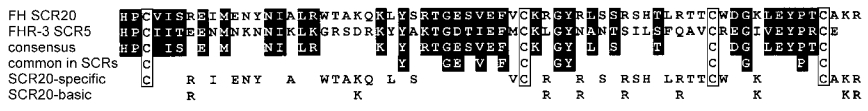

FIGURE 5. Sequence analysis of the most C-terminal domains of FH and FHR-3. To predict the residues involved in C3d binding a consensus sequence for the C3d-binding domains FH SCR20 and FHR-3 SCR5 was created (*row 3*). To exclude the residues that are structurally necessary for SCR domains in general, a frequency map of residues common in SCRs 1–18 of FH (not binding to C3d) was created as described in *Materials and Methods*. Residues common in SCRs, i.e., the same or similar residues located at the same position in at least half of FH domains, have been depicted on *row 4*. The following residues were considered similar: R and K; D and E; Y and F; T and S; I, L, A, and V; N and Q (altogether 25/67 residues). Residues specific for FH SCR20 are shown in *row 5*. Of these, putative SCR20-specific basic residues that could be involved in heparin binding are shown in *row 6*. GenBank Accession nos.: FH: CFAH,P08603; FHR-3: NP_066303,C FHR-3.

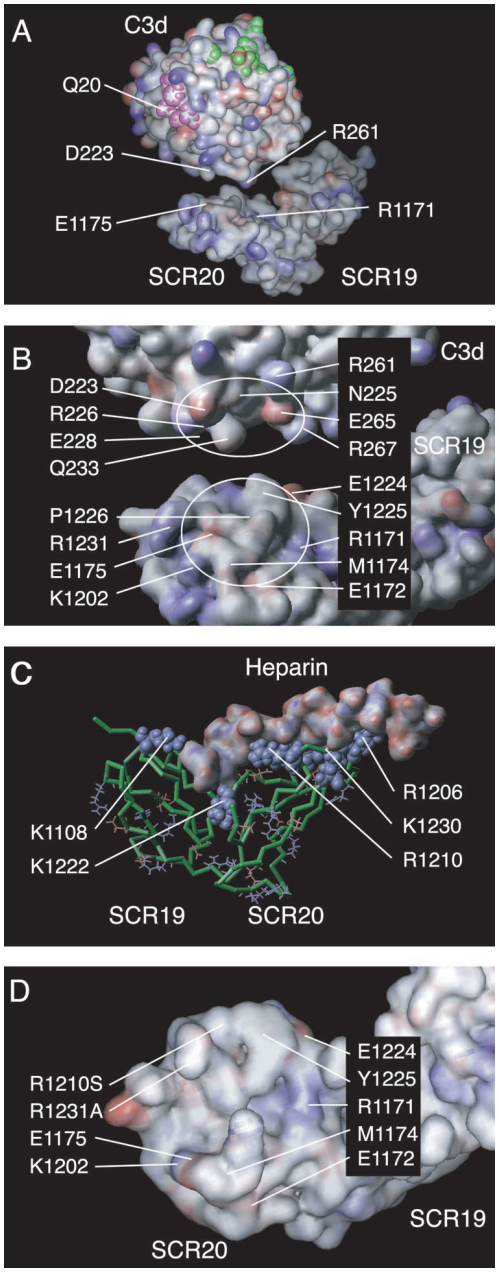

FIGURE 7. Docking analysis of FH SCR19–20 with C3d and heparin. *A* and *B*, Docking analysis of the FH SCR19–20 model to the experimentally determined structure of C3d (37) (PDB entry 1C3D) was performed manually. The site on C3d in the docking corresponds to the previously proposed areas on C3d sequence responsible for FH binding. The site on FH SCR20 that fitted best with C3d was composed of residues proposed to be involved in C3d binding by the sequence analysis (see Fig. 5). *A* and *B*, The docking result is shown with the interacting surfaces taken apart and rotated slightly backwards to reveal the surface contours and participating residues inside and around a white ring. The thioester site (Q20) is shown in pink and the CD21 binding site in green. *C*, The heparin docking analysis was performed by six separate computer-aided analyses and in each analysis heparin was positioned differently in comparison to FH SCR19–20. The docking result between FH SCR19–20 and heparin which gave the lowest potential energy after molecular dynamics simulations is shown. Heparin is displayed with a charge-colored solvent accessible surface, the FH backbone in green, the putative heparin-binding positively charged residues of FH with blue space-filling balls, and other positively charged residues of the FH model with blue side chains. *D*, A model of the mutated SCR19–20 is shown. The solvent accessible surface of the mutant FH SCR19–20 model shows changes caused by the replacement of five residues of SCR20.

FH SCR15–20: R1203E, R1206E, R1210S, K1230S, and R1231A (FH15–20 mut). It is noteworthy that the R1210 residue is often mutated in familial HUS (22). The effects of the set of mutations in the region 1203–1231 were tested by analyzing the binding of FH15–20 mut to C3d, C3b, and heparin. Analysis by surface plasmon resonance showed that the wild-type FH15–20 bound to C3d but the FH15–20 mut had lost a considerable part of its binding capacity to C3d (Fig. 8, *A* and *C*) and C3b (Fig. 8*B*). First, a biosensor chip with a high density of C3d was used. The dissociation half-life of the complex of the FH15–20 mut protein with C3d was only 34.2% (±2.95%) of that of the wild-type FH15–20.

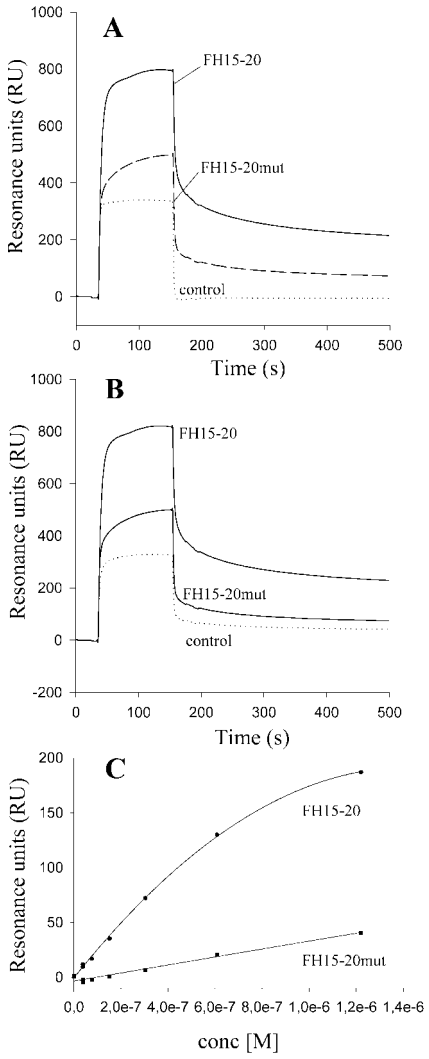

FIGURE 8. Analysis of binding of the FH SCR20 mutant construct to C3d and C3b. *A*, A mutant of the SCR15–20 construct was created by replacing five of the six basic residues forming the positively charged patch on the surface of the FH SCR19–20 model (residues 1203–1231 in FH sequence). Binding of the mutant to C3d was analyzed with a Biacore biosensor as described for Fig. 2. Nonmutated FH15–20 (solid line) and mutated FH15–20 mut (dashed line) were injected into a flowcell coupled with C3d. The binding of the wild-type protein is apparent from the distinct association and dissociation phases of the binding curve, whereas the binding of the mutant is decreased. The recombinant constructs were tested in three independent experiments each on two different chip surfaces coated with C3d, and a representative result is shown. *B*, The same experiment using C3b as a ligand. *C*, Equilibrium binding of FH15–20 vs FH15–20 mut to C3d expressed in resonance units at increasing concentrations of the analyte. A low surface density of C3d was used as described in *Materials and Methods*.

To determine rate constants for binding of FH15–20 vs the FH15–20 mut protein to C3d, a sensor chip with a low density of C3d was prepared. Under these conditions, rate constants 3.8×10^3 (1/Ms) for the association and 3.4×10^{-4} (1/s) for the dissociation phase were obtained for the wild-type FH15–20. In contrast, the binding of the mutant under these conditions was too weak to obtain reliable data. The equilibrium constants of FH15–20 binding to C3d were calculated from the rate constants as K_A of 1.1×10^7 M^{-1} and a K_D of 8.8×10^{-8}. These values are in the same range as reported earlier for the binding of the entire FH, FHR-3, and FHR-4 proteins to C3d (36). Fig. 8*C* shows a plot of the equilibrium binding concentration curve of the wild-type FH15–20 and the FH15–20 mut to C3d.

The binding of the mutant to heparin was tested by heparin-agarose affinity chromatography. To directly compare the binding, both the wild-type and the mutated FH15–20 protein were run on the heparin column at the same time. One of the proteins was radiolabeled and added in a trace amount. Its elution was monitored by the distribution of radioactivity in the elution fractions. The other unlabeled protein was added in higher quantity (30 μg) and its elution profile was followed by OD_{280}. The experiment was done by adding either the wild-type or the mutated SCR15–20 protein in the labeled form. Regardless of whether the FH15–20 mut was added in a radiolabeled (Fig. 9*A*) or unlabeled form (Fig. 9*B*), its binding to heparin was reduced as compared with the wild type. Thus, these experiments demonstrated that a group of mutations at basic residues selective for SCR20 of FH affected its interaction with heparin.

Because mutations in SCR20 reduced binding of FH15–20 to both C3d and heparin, we analyzed the structural effects of the mutations by generating a model of the mutated SCR19–20 domains. The positively charged patch that was evident in the non-mutated model could not be seen in the model of the mutant (Fig. 7*D*). In the model of the mutant the surface charges of approximately one-third of the putative C3d-binding site on SCR20 were clearly different from the wild-type model. However, the overall structure of the C3d-binding site was only little affected, thus explaining the observed residual binding of the FH15–20 mut to C3d. As expected, the putative heparin-binding site (positively charged patch) in the SCR20 domain was absent in the mutant model, but continuing from that area to the other side of SCR20 there are four additional positively charged residues (K1186, K1188, R1215, and K1222) in a row. These residues could explain the fact that the SCR20 mutant still bound to heparin, although with a decreased affinity. The additional basic residues were not within or next to the putative C3d-binding site but rather on the opposite edge of the putative C3d-binding site when compared with the mutated positively charged patch.

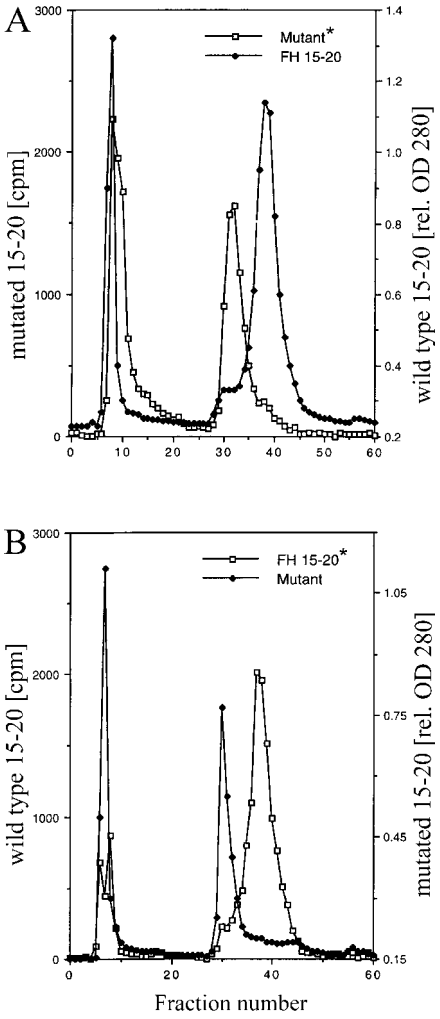

FIGURE 9. The effect of mutations in SCR20 on the binding of the FH SCR15–20 construct to heparin analyzed by heparin affinity chromatography. The mutant of FH15–20 was compared with the wild-type FH15–20 for binding to heparin. Both proteins were applied on a heparin-agarose column simultaneously and eluted by a linear salt gradient. One of the proteins was radiolabeled and added in a small amount. The elution was monitored as a migration of radioactivity (total of 20,000 cpm). The other protein was added unlabeled in a higher quantity and its elution profile was followed by OD_{280}. *A*, The FH15–20 mut protein was added in a ^{125}I-radiolabeled form and the wild type in unlabeled form. *B*, The wild-type FH15–20 was added in a radiolabeled form, and the FH15–20 mut in unlabeled form. In both cases, the binding of the mutated protein to heparin was reduced as compared with the wild type.

The relationship between C3d- and heparin-binding sites

The structural model and the reduced binding of FH15–20 mut to both C3d and heparin suggested that the C3d- and heparin-binding sites on SCR20 could be related. To test whether the two binding sites for C3b/C3d and heparin are overlapping, the binding of FH15–20 to C3b was tested in the presence of heparin (3–300 μg/ml). As shown in Fig. 10, heparin inhibited the binding of both the wild-type and the mutated protein to C3b in a dose-dependent manner. Already at the concentration of 3 μg/ml of heparin, the binding of the wild-type FH15–20 to C3b was reduced (Fig. 10*A*). In contrast, the inhibitory effect of heparin on the binding of the mutated protein to C3b was much weaker (Fig. 10*B*). In general, the binding of the FH15–20 mut protein to C3b was weaker than that of the wild-type FH15–20 due to partial deletion of the C3d-binding site (see Fig. 8). These results showed that the binding sites for C3b/C3d and heparin in the SCR20 region of FH are not independent from each other but are partially overlapping. The result is also in accordance with the modeling results shown in Fig. 7.

Discussion

In this study, we have mapped the C3d- and C3b-binding sites on FH and FHR-3 to their most C-terminal SCR domains. By mutating five basic amino acids in the SCR20 domain of the C-terminal FH15–20 construct, the binding interactions with C3d, C3b, and the polyanion heparin were significantly affected. These results show that the C-terminal C3d/C3b- and heparin-binding sites of FH are located at SCR20 and are partially overlapping. Thus, the SCR20 domain apparently has a fundamentally important role in the functions of FH. The key role of SCR20 has already been

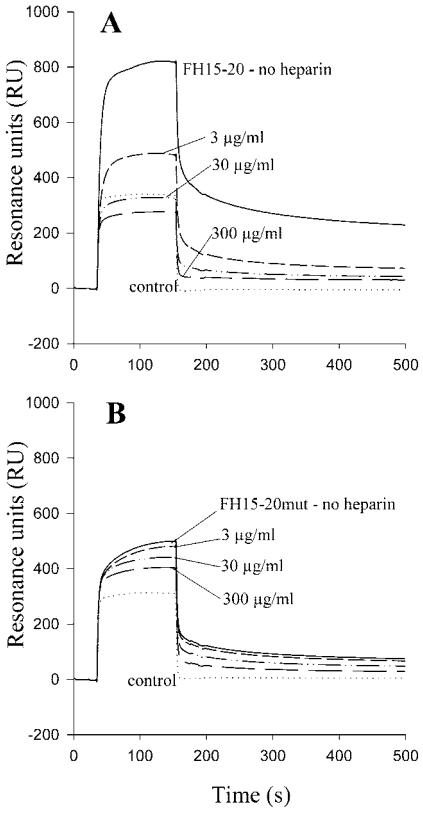

FIGURE 10. Inhibitory effect of heparin on the binding of FH15–20 to C3b. To analyze whether heparin and C3d have overlapping binding sites on SCR20 of FH, binding of either FH15–20 wild type (*A*) or the FH15–20 mut protein (*B*) to C3b was measured in the presence of different concentrations of heparin. *A,* Binding of FH15–20 to C3b was inhibited by heparin. Increasing concentrations of heparin (3–300 μg/ml) resulted in a dose-dependent reduction in FH15–20 binding to C3b. *B,* Binding of the mutated FH15–20 was in general lower compared with the wild type (see Fig. 8), and the addition of heparin has only a limited inhibitory effect. The controls (blank channel) are shown as dotted lines.

demonstrated by mutations in this region of FH in patients with familial HUS. Our results on the locations of the C3d-binding sites of FH, FHR-3, and FHR-4 at the SCR-domain level are in agreement with previous reports. A binding site for C3b on SCRs 15–20 of FH has been suggested by Sharma and Pangburn (50). Recently our analysis of the three bindings sites on FH for C3b showed that the FH region SCR19–20 binds to C3b and to its enzymatically cleaved fragment C3d (31, 51).

We show by analyzing recombinant deletion constructs of FH and FHR-3 that the C3d interaction site is in the C terminus of these proteins, i.e., in the SCR20 of FH and the SCR5 of FHR-3. With the used constructs we could not entirely exclude a role for SCR19 in binding to C3d but showed that SCR20 is essential for the interaction. Based on these results and the sequence similarities, the C3d-binding sites appear similar and in analogous positions in FH and FHR-3. To visualize the tertiary structure of the FH C terminus, a homology-based molecular model of SCR19–20 of FH was constructed on the basis of the known NMR structure of FH SCR15–16 (44). As the model structure reached a root mean square deviation plateau during the molecular dynamics simulation, it represents one possible overall conformation for this pair of SCR domains. However, as the angle between two SCRs is considered to be highly flexible (52), we considered the rotation and torsion angles between SCR19 and SCR20, and thus the hinge region structure in general, as only one of the possible conformations. Because our deletion constructs FH SCR15–19 and FHR-3 SCR1–4 did not bind to heparin or C3d at all, the last SCR is obligatory for these interactions. Thus, it is unlikely that SCR19 of FH or SCR4 of FHR-3 contribute to the interactions to any great extent.

By sequence alignment, we identified 24 residues that were shared by the C3d-binding domains of FH and FHR-3 but absent from the other SCR domains of these proteins. The positions of the putative C3d-binding consensus residues in the tertiary molecular model structure of FH SCR19–20 showed that 12 of them formed a patch on the surface. When docked manually with the known structure of C3d, eight of these residues were found on the best docking surface area (Fig. 7*B*). In addition, three charged residues were found within the putative C3d-binding area and none of them was found in FHR-3 (R1171, E1175, and R1231). However, some other charged residues on FHR-3 might compensate for this difference by taking a similar location. For example, the possible role of the FH residue E1175 could be compensated for by a spatially closely located Glu residue in FHR-3 corresponding to FH A1229.

The recently determined tertiary structure of C3d (37) revealed the locations of the previously reported C3d sequences that were suggested to be responsible for the binding to FH by Lambris and colleagues (49, 53, 54). The proposed sequences were based on the inhibition of C3d-FH interaction by peptides spanning the C-terminal part of C3d. The proposed two sequences form two neighboring loops on the surface of the C3d tertiary structure, in about a 90° angle from the thioester site and clearly distinct from the CD21 (CR2) binding site (37, 48). In our docking analysis, this proposed site on C3d gave the best fit for our putative C3d-binding site on FH SCR20. The charges and contours on the two surfaces seem to be complementary to each other. The in silico docking analysis, used in this study as a tool for visualizing and predicting the interaction between FH and C3d, is in good agreement with the experimental data that we obtained using the SCR15–20 mutant.

A mutant of the FH fragment SCR15–20 was constructed by using site-directed mutagenesis. A total of five positively charged amino acid residues was replaced with neutral or differently charged residues (R/S, K/S, and R/E) to avoid introduction of a new hydrophobic patch. The created mutant seemed to fold properly since mAbs known to be specific for SCR20 of FH (30) bound to it (data not shown). Surface plasmon resonance analyses showed that binding of the mutated protein to C3d was reduced to one-third of that of the nonmutated FH15–20 when a high surface density of C3d was used. At a lower density of C3d, binding was almost completely abrogated. Heparin affinity chromatography showed that the heparin-binding capacity of the mutant was decreased as well. These data indicate that residues within the same positively charged patch are involved in both heparin and C3d binding, and that for both of these interactions SCR20 is needed. However, because a total of five residues were mutated simultaneously, it is possible that not all of them are relevant for the interaction with C3d. Replacement or mutation of additional amino acids in the C terminus of FH could have led to a complete lack of binding to C3d and heparin. However, in a pathophysiological context like atypical HUS (21–23), a partial reduction in the activity of FH, as shown in this work, seems to be sufficient for the development of the disease.

The results from the analyses with the FH15–20 mut showing partially overlapping binding sites on FH SCR20 for heparin and C3d fit well with the molecular modeling results. It is likely that the mutated positively charged patch is involved in the putative heparin-binding site found in the docking analysis. This is because five of six residues were involved in the best fit of the docking

analysis between SCR19–20 and heparin. However, other interaction analyses have shown that complementarity of structures does not always reveal the residues critical for the interaction (55). The work of Szakonyi et al. (48) recently showed that complementary structures and SCR side-chain interactions seem to be responsible for binding of CD21 to C3d. The whole positively charged patch in SCR20 of FH is probably not necessary for C3d binding since FHR-3 that binds to C3d has only one of the six positively charged residues. The mutated positively charged patch in the model is on the border of the putative C3d-binding site. Thus, the mutations have probably changed the conformation of the C3d-binding site enough to restrict the interaction. This is also suggested by the molecular modeling analysis of the FH SCR19–20 structure where the amino acid changes had been made before the energy minimizations (Fig. 7*D*). Very recently, another computer model on the C-terminal domains of FH was presented (56). Solely based on a theoretical approach, the authors suggested that a heparin-binding site composed of four positively charged residues is located at a position different from our proposal. Positively charged residues corresponding to three of those residues are also found at the same location in the primary structure of the C-terminal domains of both FHR-3 and FHR-4, and according to our experimental results, FHR-4 does not bind to heparin at all, and the heparin-binding site of FHR-3 is within SCR1–3. Thus, although it might be possible that residues from a larger region in SCR20 contribute to heparin binding, the model presented in this study appears more consistent with the existing experimental data. Further analysis is necessary to show how much the individual amino acids contribute to the interaction.

The cofactor, decay-accelerating and competing functions of FH need to be restricted to nonactivator surfaces to prevent progression of AP activation. Although the detailed mechanism for this discrimination remains to be revealed, it is possible that SCR20 is involved in this process. Our results, together with the work of Blackmore et al. (29) indicate that in addition to binding to C3d, the SCR20 domain also binds to polyanions (51). The covalent surface-attachment site on C3d is located ~30 Å away from the suggested FH-binding site. This suggests that the FH-binding site is located close to the target surface structures such as glycosaminoglycans or terminal sialic acids on membrane glycoproteins on nonactivator surfaces. SCR20 of FH could be involved in the discrimination process by recognizing nonactivator structures either directly or in combination with C3b/C3d. It is possible that the AP discrimination occurs by a joint recognition because the C3d-binding and heparin-binding sites are partially overlapping. In contrast, because heparin inhibited the binding of FH15–20 to C3d, the two surface-attached ligands, polyanions and C3d, might offer alternative ligands for FH binding. If the C3d epitope is hidden on surface-associated C3b, its role as a FH-binding site could be taken by surface polyanions.

Recently, mutations in FH have been reported in patients with familial HUS (21, 22). The C terminus of FH, and SCR20 in particular, is a hot spot for mutations associated with this disease. The point mutations described in HUS patients (positions R1210 and R1215) are included in the FH SCR15–20 mutant presented in this study or are very close to the proposed binding sites. It is likely that changes in the ability of FH to bind to cell surfaces or to C3b/C3d contribute to the pathogenesis of the disease. The fact that two important binding sites are located at the very C-terminal end of the FH molecule implies that the interaction of FH with C3b is very dynamic. Because FH is a longitudinal and flexible molecule (52), the C-terminal SCR20 might be an essential contact point of FH with C3b and cellular surface structures. In HUS, this function could be abrogated and control of the AP activation on the self surfaces of erythrocytes, platelets, and endothelial cells could be disturbed.

Acknowledgments

We thank Marjatta Ahonen and Gerlinde Heckrodt for expert technical assistance, Dr. Jana Thamm for protein purification, and Dr. Hilkka Lankinen (Department of Virology, Haartman Institute and Helsinki University Central Hospital, University of Helsinki, Helsinki, Finland) for support with the Biacore instrument.

References

1. Walport, M. J. 2001. Complement: first of two parts. *N. Engl. J. Med. 344:1058.*
2. Müller-Eberhard, H. J., and R. D. Schreiber. 1980. Molecular biology and chemistry of the alternative pathway of complement. *Adv. Immunol. 29:1.*
3. Pangburn, M. K., D. C. Morrison, R. D. Schreiber, and H. J. Müller-Eberhard. 1980. Activation of the alternative complement pathway: recognition of surface structures on activators by bound C3b. *J. Immunol. 124:977.*
4. Fearon, D. T., and K. F. Austen. 1975. Properdin: binding to C3b and stabilization of the C3b-dependent C3 convertase. *J. Exp. Med. 142:856.*
5. Fearon, D. T., and K. F. Austen. 1975. Initiation of C3 cleavage in the alternative complement pathway. *J. Immunol. 115:1357.*
6. Müller-Eberhard, H. J. 1986. The membrane attack complex of complement. *Annu. Rev. Immunol. 4:503.*
7. Morgan, B. P., and S. Meri. 1994. Membrane proteins that protect against complement lysis. *Springer Semin. Immunopathol. 15:369.*
8. Liszewski, M. K., T. C. Farries, D. M. Lublin, I. A. Rooney, and J. P. Atkinson. 1996. Control of the complement system. *Adv. Immunol. 61:201.*
9. Reid, K. B., and A. J. Day. 1989. Structure-function relationships of the complement components. *Immunol. Today 10:177.*
10. DiScipio, R. G. 1992. Ultrastructures and interactions of complement factors H and I. *J. Immunol. 149:2592.*
11. Whaley, K., and S. Ruddy. 1976. Modulation of the alternative complement pathways by β1H globulin. *J. Exp. Med. 144:1147.*
12. Weiler, J. M., M. R. Daha, K. F. Austen, and D. T. Fearon. 1976. Control of the amplification convertase of complement by the plasma protein β1H. *Proc. Natl. Acad. Sci. USA 73:3268.*
13. Pangburn, M. K., R. D. Schreiber, and H. J. Müller-Eberhard. 1977. Human complement C3b inactivator: isolation, characterization, and demonstration of an absolute requirement for the serum protein β1H for cleavage of C3b and C4b in solution. *J. Exp. Med. 146:257.*
14. Fearon, D. T. 1978. Regulation by membrane sialic acid of β1H-dependent decay-dissociation of amplification C3 convertase of the alternative complement pathway. *Proc. Natl. Acad. Sci. USA 75:1971.*
15. Zipfel, P. F., and C. Skerka. 1999. FHL-1/reconectin: a human complement and immune regulator with cell-adhesive function. *Immunol. Today 20:135.*
16. Meri, S., V. Koistinen, A. Miettinen, T. Tornroth, and I. J. Seppala. 1992. Activation of the alternative pathway of complement by monoclonal λ light chains in membranoproliferative glomerulonephritis. *J. Exp. Med. 175:939.*
17. Hogasen, K., J. H. Jansen, T. E. Mollnes, J. Hovdenes, and M. Harboe. 1995. Hereditary porcine membranoproliferative glomerulonephritis type II is caused by factor H deficiency. *J. Clin. Invest. 95:1054.*
18. Ault, B. H., B. Z. Schmidt, N. L. Fowler, C. E. Kashtan, A. E. Ahmed, B. A. Vogt, and H. R. Colten. 1997. Human factor H deficiency: mutations in framework cysteine residues and block in H protein secretion and intracellular catabolism. *J. Biol. Chem. 272:25168.*
19. Pickering, M. C., H. T. Cook, J. Warren, A. E. Bygrave, J. Moss, M. J. Walport, and M. Botto. 2002. Uncontrolled C3 activation causes membranoproliferative glomerulonephritis in mice deficient in complement factor H. *Nat. Genet. 31:424.*
20. Jokiranta, T. S., A. Solomon, M. K. Pangburn, P. F. Zipfel, and S. Meri. 1999. Nephritogenic λ light chain dimer: a unique human miniautoantibody against complement factor H. *J. Immunol. 163:4590.*
21. Richards, A., M. R. Buddles, R. L. Donne, B. S. Kaplan, E. Kirk, M. C. Venning, C. L. Tielemans, J. A. Goodship, and T. H. Goodship. 2001. Factor H mutations in hemolytic uremic syndrome cluster in exons 18–20, a domain important for host cell recognition. *Am. J. Hum. Genet. 68:485.*
22. Perez-Caballero, D., C. Gonzalez-Rubio, M. E. Gallardo, M. Vera, M. Lopez-Trascasa, S. Rodriguez de Cordoba, and P. Sanchez-Corral. 2001. Clustering of missense mutations in the C-terminal region of factor H in atypical hemolytic uremic syndrome. *Am. J. Hum. Genet. 68:478.*
23. Caprioli, J., P. Bettinaglio, P. F. Zipfel, B. Amadei, E. Daina, S. Gamba, C. Skerka, N. Marziliano, G. Remuzzi, and M. Noris. 2001. The molecular basis of familial hemolytic uremic syndrome: mutation analysis of factor H gene reveals a hot spot in short consensus repeat 20. *J. Am. Soc. Nephrol. 12:297.*
24. Pangburn, M. K., and H. J. Müller-Eberhard. 1978. Complement C3 convertase: cell surface restriction of β1H control and generation of restriction on neuraminidase-treated cells. *Proc. Natl. Acad. Sci. USA 75:2416.*
25. Kazatchkine, M. D., D. T. Fearon, and K. F. Austen. 1979. Human alternative complement pathway: membrane-associated sialic acid regulates the competition between B and β1H for cell-bound C3b. *J. Immunol. 122:75.*
26. Meri, S., and M. K. Pangburn. 1990. Discrimination between activators and nonactivators of the alternative pathway of complement: regulation via a sialic acid/polyanion binding site on factor H. *Proc. Natl. Acad. Sci. USA 87:3982.*
27. Pangburn, M. K., M. A. Atkinson, and S. Meri. 1991. Localization of the heparin-binding site on complement factor H. *J. Biol. Chem. 266:16847.*

28. Blackmore, T. K., T. A. Sadlon, H. M. Ward, D. M. Lublin, and D. L. Gordon. 1996. Identification of a heparin binding domain in the seventh short consensus repeat of complement factor H. *J. Immunol. 157:5422.*
29. Blackmore, T. K., J. Hellwage, T. A. Sadlon, N. Higgs, P. F. Zipfel, H. M. Ward, and D. L. Gordon. 1998. Identification of the second heparin-binding domain in human complement factor H. *J. Immunol. 160:3342.*
30. Prodinger, W. M., J. Hellwage, M. Spruth, M. P. Dierich, and P. F. Zipfel. 1998. The C-terminus of factor H: monoclonal antibodies inhibit heparin binding and identify epitopes common to factor H and factor H-related proteins. *Biochem. J. 331:41.*
31. Jokiranta, T. S., J. Hellwage, V. Koistinen, P. F. Zipfel, and S. Meri. 2000. Each of the three binding sites on complement factor H interacts with a distinct site on C3b. *J. Biol. Chem. 275:27657.*
32. Ram, S., A. K. Sharma, S. D. Simpson, S. Gulati, D. P. McQuillen, M. K. Pangburn, and P. A. Rice. 1998. A novel sialic acid binding site on factor H mediates serum resistance of sialylated *Neisseria gonorrhoeae*. *J. Exp. Med. 187:743.*
33. Hellwage, J., T. Meri, T. Heikkilä, A. Alitalo, J. Panelius, P. Lahdenne, I. J. Seppälä, and S. Meri. 2001. The complement regulator factor H binds to the surface protein OspE of *Borrelia burgdorferi*. *J. Biol. Chem. 276:8427.*
34. Zipfel, P. F., T. S. Jokiranta, J. Hellwage, V. Koistinen, and S. Meri. 1999. The factor H protein family. *Immunopharmacology 42:53.*
35. McRae, J. L., P. J. Cowan, D. A. Power, K. I. Mitchelhill, B. E. Kemp, B. P. Morgan, and B. F. Murphy. 2001. Human factor H-related protein 5 (FHR-5): a new complement-associated protein. *J. Biol. Chem. 276:6747.*
36. Hellwage, J., T. S. Jokiranta, V. Koistinen, O. Vaarala, S. Meri, and P. F. Zipfel. 1999. Functional properties of complement factor H-related proteins FHR-3 and FHR-4: binding to the C3d region of C3b and differential regulation by heparin. *FEBS Lett. 462:345.*
37. Nagar, B., R. G. Jones, R. J. Diefenbach, D. E. Isenman, and J. M. Rini. 1998. X-ray crystal structure of C3d: a C3 fragment and ligand for complement receptor 2. *Science 280:1277.*
38. Eggertsen, G., U. Hellman, A. Lundwall, J. Folkersen, and J. Sjoquist. 1985. Characterization of tryptic fragments of human complement factor C3. *Mol. Immunol. 22:833.*
39. Koistinen, V., S. Wessberg, and J. Leikola. 1989. Common binding region of complement factors B, H and CR1 on C3b revealed by monoclonal anti-C3d. *Complement Inflamm. 6:270.*
40. Kyhse-Andersen, J. 1984. Electroblotting of multiple gels: a simple apparatus without buffer tank for rapid transfer of proteins from polyacrylamide to nitrocellulose. *J. Biochem. Biophys. Methods 10:203.*
41. Hellwage, J., C. Skerka, and P. F. Zipfel. 1997. Biochemical and functional characterization of the factor-H-related protein 4 (FHR-4). *Immunopharmacology 38:149.*
42. Kühn, S., and P. F. Zipfel. 1995. The baculovirus expression vector pBSV-8His directs secretion of histidine-tagged proteins. *Gene 162:225.*
43. Jokiranta, T. S., J. Westin, U. R. Nilsson, B. Nilsson, J. Hellwage, S. Löfas, D. L. Gordon, K. N. Ekdahl, and S. Meri. 2001. Complement C3b interactions studied with surface plasmon resonance technique. *Int. J. Immunopharmacol. 1:495.*
44. Barlow, P. N., A. Steinkasserer, D. G. Norman, B. Kieffer, A. P. Wiles, R. B. Sim, and I. D. Campbell. 1993. Solution structure of a pair of complement modules by nuclear magnetic resonance. *J. Mol. Biol. 232:268.*
45. Jokiranta, T. S., J. Tissari, O. Teleman, and S. Meri. 1995. Extracellular domain of type I receptor for transforming growth factor-β: molecular modelling using protectin (CD59) as a template. *FEBS Lett. 376:31.*
46. Galloway, S. M., K. P. McNatty, L. M. Cambridge, M. P. Laitinen, J. L. Juengel, T. S. Jokiranta, R. J. McLaren, K. Luiro, K. G. Dodds, G. W. Montgomery, et al. 2000. Mutations in an oocyte-derived growth factor gene (BMP15) cause increased ovulation rate and infertility in a dosage-sensitive manner. *Nat. Genet. 25:279.*
47. Zipfel, P. F., and C. Skerka. 1994. Complement factor H and related proteins: an expanding family of complement-regulatory proteins? *Immunol. Today 15:121.*
48. Szakonyi, G., J. M. Guthridge, D. Li, K. Young, V. M. Holers, and X. S. Chen. 2001. Structure of complement receptor 2 in complex with its C3d ligand. *Science 292:1725.*
49. Lambris, J. D., D. Avila, J. D. Becherer, and H. J. Müler-Eberhard. 1988. A discontinuous factor H binding site in the third component of complement as delineated by synthetic peptides. *J. Biol. Chem. 263:12147.*
50. Sharma, A. K., and M. K. Pangburn. 1996. Identification of three physically and functionally distinct binding sites for C3b in human complement factor H by deletion mutagenesis. *Proc. Natl. Acad. Sci. USA 93:10996.*
51. Jokiranta, T. S., J. Hellwage, M. Friese, P. F. Zipfel, and S. Meri. 2000. Identification of the binding site on factor H SCR 20 for C3d. *Immunopharmacology 49:44. (Abstr.).*
52. Aslam, M., and S. J. Perkins. 2001. Folded-back solution structure of monomeric factor H of human complement by synchrotron x-ray and neutron scattering, analytical ultracentrifugation and constrained molecular modelling. *J. Mol. Biol. 309:1117.*
53. Becherer, J. D., J. Alsenz, I. Esparza, C. E. Hack, and J. D. Lambris. 1992. Segment spanning residues 727–768 of the complement C3 sequence contains a neoantigenic site and accommodates the binding of CR1, factor H, and factor B. *Biochemistry 31:1787.*
54. Lambris, J. D., Z. Lao, T. J. Oglesby, J. P. Atkinson, C. E. Hack, and J. D. Becherer. 1996. Dissection of CR1, factor H, membrane cofactor protein, and factor B binding and functional sites in the third complement component. *J. Immunol. 156:4821.*
55. Clackson, T., and J. A. Wells. 1995. A hot spot of binding energy in a hormone-receptor interface. *Science 267:383.*
56. Perkins, S. J., and T. H. Goodship. 2002. Molecular modelling of the C-terminal domains of factor H of human complement: a correlation between haemolytic uraemic syndrome and a predicted heparin binding site. *J. Mol. Biol. 316:217.*